ANALYSIS OF PEDESTRIAN-TRAM COLLISION PHENOMENA: POSSIBILITIES OF SIMULATION MODELS VALIDATION

ROMAN JEZDIK[1,3], VOJTECH RULC[2,3], PETR KUBOVY[3], VLADISLAV KEMKA[4], JAN KOVANDA[4], BARBORA MLEJNKOVA[5], TOMMY TIKKANEN[6]

[1]VUKV a. s., Research, development, and testing of railway rolling stock, Prague, Czech Republic

[2]Advanced Engineering, s.r.o. , Prague, Czech Republic

[3]Department of Anatomy and biomechanics, Faculty of Physical Education and Sport, Charles University, Prague, Czech Republic

[4]Regional Technology Institute, University of West Bohemia, Pilsen, Czech Republic

[5]SKODA TRANSPORTATION a. s., Pilsen, Czech Republic

[6]GIM Oy, Espoo, Finland

DOI: 10.17973/MMSJ.2023_06_2023043

jezdik@vukv.cz

The article deals with the validation of the pedestrian simulation model as the initial study for future virtual testing of the tram front-end. The vision of virtual modeling approval is the main motivation of the study. The biofidelity of existing models was the subject of volunteer tests. The data are utilized for assessment of both adapted real anthropomorphic test device and presented simulation models created by means of commercial computer systems LS-DYNA and RADIOSS.

Two basic tram front-end geometry were used in the pedestrian collision simulations. The resulting physical data are presented. The article demonstrates the complexity of the problem under study [Margaritis 2007] and confirms the correctness of the segment testing used in the automotive area.

KEYWORDS

Anthropomorphic test device, crash test dummy, computer simulation models, biofidelity, simulation model validation, evaluation of tram-pedestrian crash, tram front end, injury criteria

1 INTRODUCTION

Currently, a new standard regulating vehicle end design for trams and light rail vehicles with respect to pedestrian safety is under preparation [CEN/TC 256 2020]. The standard expects using of a validated ATD (=anthropomorphic test device, generally called “crash test dummy”) [Wismans 2014], [Wismans 2000] simulation model to evaluate front-end influence on the pedestrian where the ATD is standing sideways to the tram front. A validation process of the ATD simulation model against existing physical ATD was proposed and practically performed to meet this aim. Commercially available ATD models are considered because the meeting of the new standard requirement should not be limited to software development capabilities of ATD simulation model modification.

At the beginning of this work, there was a physical ATD JASTI in a sitting position [LS-Dyna 2023b] (Hybrid-III50th Percentile Male ATD certificated for front impact) in ownership of the Department of Anatomy and biomechanics, Faculty of Physical Education and Sport, Charles University. The mentioned ATD was equipped by the pedestrian kid to provide a physical ATD in a standing position, but without certification. Therefore, some tests to compare the mechanical behavior of the physical standing ATD and physical human were performed [Tomsovsky 2022]. In parallel, human body models (HBM) are developed.

As a next step of work, a series of physical standing ATD collision tests impacted by a tram were performed [Tomsovsky 2019]. Front and side impacts were performed using five types of trams. Impact velocities of 5, 10, 15, and 20 km/h as the initial conditions [Kovanda 2021] were considered. Contemporaneously, finite element simulation models of these collision tests were prepared, and appropriate simulations were provided. Comparing of the results is given below. LS-Dyna solver and Radios solver incl. appropriate ADT simulation models were used. Some additional tests of the tram laminated structures [Jezdik 2021] and windscreen glass [Jezdik 2019] were provided to obtain the correct properties for modeling.

2 ATD AND ITS MODELS

2.1 *Physical ATD*

Only one Hybrid-III-50th Percentile Male ATD with a Pedestrian kit from Jasti was available for the entire research, see fig. 1. It is therefore an ATD representing a pedestrian and intended primarily for frontal impacts, it is 172 cm tall and weighs 80 kg. The ATD passed certification [Jasti 2015] in a sitting position before measurements and after the replacement of parts damaged during tests. The ATD is fitted with built-in calibrated 3D inertial sensors, 3D dynamometric load cells, and a DTI acquisition system from Kistler. The total weight of the ATD, as well as their individual segments, remained intact even when the measuring devices were installed. CrashDesigner software was used to record and process measured data. 3-axis accelerometers and gyroscopes were placed in the ATD approximately at the centers of gravity of the head, chest, and pelvis. Furthermore, 3-axis force meters and torque meters in the areas of the spine C1, C7, Th8, and S5, the centers of the femurs, and the distal ends of the tibias. The entire system recorded data at a frequency of 20 kHz, for up to 1 minute. Just before each measurement, the sensors were always balanced in the vertical position of the ATD and always also measured in the static horizontal position, for the possibility of calculating the absolute values of a load of individual segments. No hardware or software filters were applied to the recording prior to the calculation of the evaluation parameters.

Two portable 3D dynamometers 9286BA with a scanning frequency of 20 kHz were also used for accurate recording of the reaction forces between the surface and the ATD.

The kinematics of the ATD's movement were recorded by the Qualisys 3D mocap system (500 fps) and two high-speed cameras Photron SA-X2 - 10,000 fps (sagittal view, Nikkor lens 50/f1.2) and Redlake HG-100k - 1000 fps (dorsal view, Nikkor lens 500/f4).

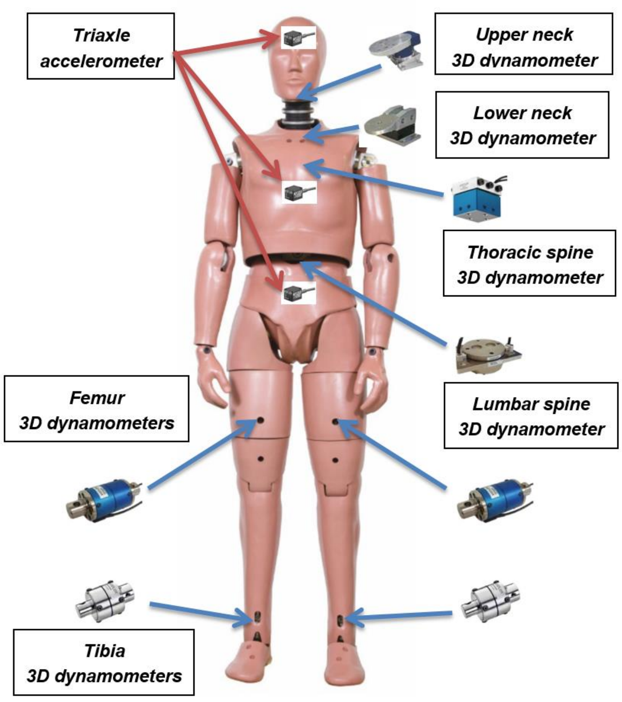

Figure 1. Hybrid III 50th Percentile Male Pedestrian ATD. Source: [Jasti 2023]

As already described above, our ATD is intended primarily for frontal impacts in a sitting position, for which it is also calibrated. As a frequent case of a collision between a tram and a pedestrian is also a side impact (see [Tomsovsky 2019] and [Tomsovsky 2022]), it was advisable to carry out validation experiments for this case as well. To increase the credibility of this process (biofidelity), we also validated the side impact ATD by comparing it with live probands. For obvious reasons, these experiments were performed only for low loads. The principle of validation consisted in the identical impact loading of the manikin and live probands. The load was implemented with a pendulum impactor weighing 5 kg and 4-speed levels, but a maximum of 2 m/s. Validation was performed for side and frontal impacts as well, see fig. 2. The recordings of the same accelerometers placed at the back of the head and Th8 on the spine were compared. 20 living probands participated in the study. Impact loads to the forehead and side of the head, shoulder, and thigh from the side and chest from the front were compared. The rated parameters were the maximum achieved acceleration values and values corresponding to HIC calculations from the recording of both 3-axis accelerometers (MMF KS963B100, Dewesoft Sirius acquisition, acquisition frequency 20 kHz). The maximum acceleration values of the head and chest were 30 to 50 % higher for ATD for all impacts to the head, chest, and thighs. When using the HIC comparison criterion, the differences were even lower. A surprising exception is the case of impact to the upper arm from the side, where the results of the ATD and the live probands are almost identical. In particular, the results show that the ATD has the same properties for side and front impacts, so it is also applicable for our side crash tests. But overall, the ATD is slightly stiffer with lower damping capabilities. The estimated damage to living creatures will most likely be lower than crash tests with our ATD prediction. The results of the experiments will be published in the near future. The study contributes to road safety in terms of [Safety conference 2020] in terms of more profound knowledge of injury mechanisms and the influence of the vehicle structure. The aim of the Stockholm Declaration is to reduce the number of fatalities to 50 % in 2030 compared to 2020.

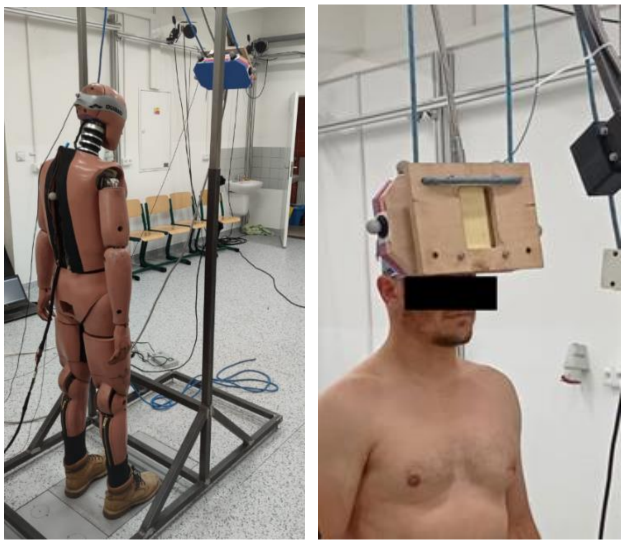

Figure 2. Hybrid III 50th Percentile Male Pedestrian ATD (not certificated) and proband

2.2 *ATD simulation model in LS-Dyna*

The LSTCH3.103008 V1. RigidFE 50th model of the standing ATD was used. The total mass of the model is 78.7 kg (calculated by preprocessor Ansa). Fig. 3 shows the entire ATD model and parts of the ATD model modeled using individual materials. It is possible to see that rigid material (*MAT_RIGID) is used to take into account limbs, pelvis, collar bones, and vertebrae. Elastic material (*MAT_ELASTIC) is used for modeling soft tissues of limbs and the chest area around the neck. Low-density foam material (*MAT_LOW_DENSITY_FOAM) represents soft tissues of the knees, chest, and pelvis surface. The stiffness of the head and chest piece is represented by viscoelastic material (*MAT_VISCOELASTIC). Parts modeled by plastic material with kinematic hardening (*MAT_PLASTIC_KINEMATICS) reinforce ribs and represents ATD shoes. Null (*MAT_NULL) material is used for contact on the neck and chest surfaces.

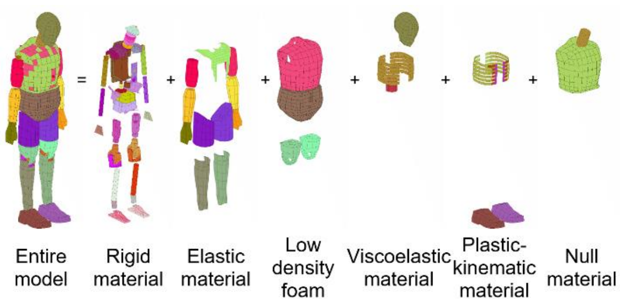

Figure 3. Entire LS-Dyna ATD model and parts of the ATD model modeled using individual materials

Revolute joints (*CONSTRAINED_JOINT_REVOLUTE) are used to simulate vertebrae connections (cranium-C1, C7-Th1), shoulder joints, and connection of the collarbone to the sternum. Spherical joints (*CONSTRAINED_JOINT_SPHERICAL) are used as intervertebral, elbow, knee wrist, and ankle joints. Translational movements of chest parts are represented by means of *CONSTRAINED_JOINT_TRANSLATIONAL. Stiffness of joints is considered as generalized via *CONSTRAINED_JOINT_SSTIFFNES_GENERALIZED keyword. Automatic contact definitions (*CONTACT_AUTOMATIC_SURFACE_TO_SURFACE) are used for parts in potential contact.

2.3 *ATD simulation model in Radioss*

For the Radioss solver, a standard Radioss ATD of a 50th percentile male (see fig. 4) was used and modified based on the impact tests performed. The weight of the individual parts of the simulation ATD model was adjusted based on the weight of the physical ATD parts, resulting in a total weight of 79.0 kg. The main skeleton of the simulation ATD model which attaches the muscle element to itself is made up of rigid elements RBE2. The muscle part of the simulation ATD model is modeled with visco-elastic foam using a generalized Maxwell-Kelvin-Voigt model where the viscosity is based on the Navier equations. The whole simulation ATD model is covered with skin. It is a 2D element with a Johnson-Cook material model. There are no muscle elements on the palms below the surface elements, which is compensated by the choice of a stiffer material. The skin element originally used at the joint locations has been removed based on validation work to be more faithful to the stiffness of the joints. Conversely, a joint mechanism was inserted between the previously rigidly joined thoracic and pelvic parts.

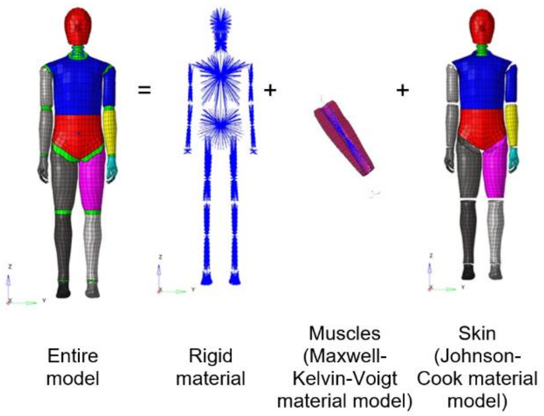

Figure 4. Entire RADIOSS ATD model and parts of the ATD model modeled using individual materials

The stiffness of individual joints was subjected to very intensive validation, and a strongly non-linear characteristic was chosen in all cases.

3 COLLISION SCENARIOS

The collision scenarios was based on the scenario A given in the technical report [CEN/TC 256 2020]. There is prescribed a lateral collision of a tram front end towards the impacted standing pedestrian (50th percentile male ATD) in the report [CEN/TC 256 2020]. A front impact is also considered as the ATD is primary designed for this orientation. The collision speed of 20 km/h prescribed in [CEN/TC 256 2020] is considered as the maximum one.

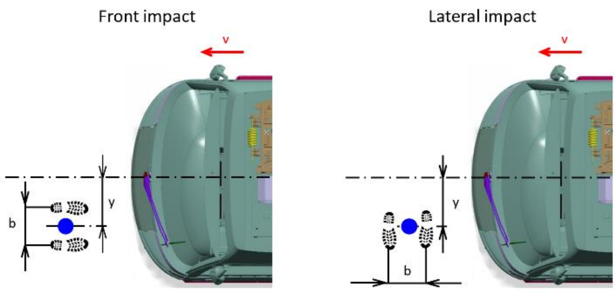

Figure 5. Collision scenarios under consideration. Blue point is the ATD center of gravity projection

Two collision scenarios were tested and modeled, see fig. 5. The first was the front impact, the second was the side impact where the ATD left shoulder is oriented to the tram. Impact velocities v = 5, 10, 15 and 20 km/h were considered. The distance of ATD center of gravity projection (the blue point in fig. 5) towards the axis of the track is denoted by letter y. The lateral distance of ATD shoes is marked with b.

4 REAL TESTS WITH PHYSICAL ATD

Five tram types were available for real tests in Prague Transport Company (DPP): 14T, 15T, T3, KT8 and T6. From the point of view of this project, the type T6 is similar to the type KT8. Moreover, the type T6 was decommissioned in Prague during realization of this project. The full test program was realized for types 14T, 15T, T3, KT8, but it was reduced for the type T6 due to this reason.

Real tests were carried out on the test track of DPP yard in Prague-Hostivar. One front and one lateral impact were realized for each of the four above-mentioned velocities. Accelerometers and gyroscopes were used to record the behavior of head, chest, and pelvis center of gravity. Vertebrae (C1, C7, TH5, L5, and S5), femurs, and ankles were equipped with load cells. The ATD was supported by a load cell plate to identify reaction components due to the ground in the initial position. The motion of the ATD was recorded by two high-speed cameras (front and lateral view) and by QUALISIS system. The system monitors trajectories of markers (small balls) connected to the observed object (the ATD and the tram) via a set of cameras.

Fig. 6 shows the ADT prepared in position on the front impact by T3 type tram (left) and on the lateral impact by 14T type tram (right). The data cable connected to the ATD was disconnected just before the impact.

Figure 6. Examples of test setup (before disconnecting of the ATD data cable). T3 – front impact (left), 14T – lateral impact (right)

5 SIMULATIONS

Two numerical models were used to simulate each of the above-mentioned impacts. The finite element method with explicit time integration was used in both cases.

The first numerical model (= Model 1) was provided by means of LS-Dyna solver [LS-Dyna 2023a]. The ATD model described in par. 2.2 was used for simulations. Models of individual trams' front ends were prepared via ANSA preprocessor for the first model.

The second numerical model (= Model 2) was provided by means of Radioss solver [Altair 2023]. The ATD model described in par. 2.3 was used for simulations. Individual trams' front ends were prepared via HYPERMESH for the second model.

The parts of the tram front end surfaces influencing contact with the ATD model were considered as deformable. Other parts of high stiffness were modeled in a simplified manner as a rigid body. The influence of gravity acceleration was respected in simulations.

There are shown Model 1 (used for T3 tram front impact simulation) and Model 2 (used for 14T tram lateral impact simulation) as examples in fig. 7.

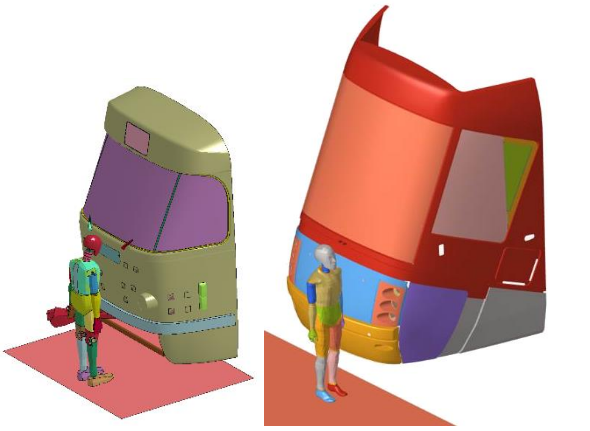

Figure 7. Examples of simulation models. Model 1 used for T3 tram front impact simulation (left) and Model 2 used for 14T tram lateral impact simulation (right)

6 RESULTS

For purposes of the validation, the T3 tram type was selected as a representative of the old tram front-end design, i.e. design with a negative front contour slope of the lower half. Similarly, the 14T tram type was selected as a representative of modern tram front-end design, i.e. design with mainly positive front contour slope. See fig. 8.

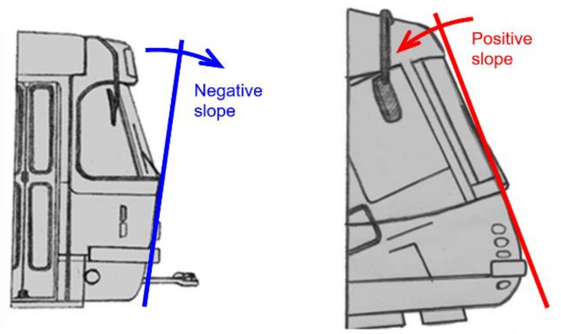

Figure 8. T3 (left) and 14T (right) frontend slope

There are presented accelerations in the following graphs obtained by testing and numerical simulation via Model 1 and Model 2, respectively.

Local acceleration component x (longitudinal component) of the head is presented in the case of the front impact, see fig. 9 and 11. The signals were shifted in time with respect to each other to have aligned their peaks of head acceleration. Local acceleration component y (lateral component) of the pelvis is presented in the case of the lateral impact, see fig. 10 and 12. The signals were shifted in time with respect to each other to have aligned their peaks of pelvis acceleration. Both acceleration signals from tests and acceleration signals from simulation were filtered by a 300 Hz lowpass filter.

Head performance criterion was evaluated for the acceleration component x for the front impact, see tab. 1 and 6. HPC was used as a tool for signal comparison in this case. The results of HIC (volunteers) and HPC (ATD) correlate well in the low level of AIS (Abbreviated Injury Scale) and there is a presumption of the close bond even of real injury level [Hozman 2014, 2017]. Moreover, peaks of the acceleration components and correlation coefficients are presented for front impact in tables 2, 3, 7 and 8, for lateral impact in tables 4, 5, 9 and 10.

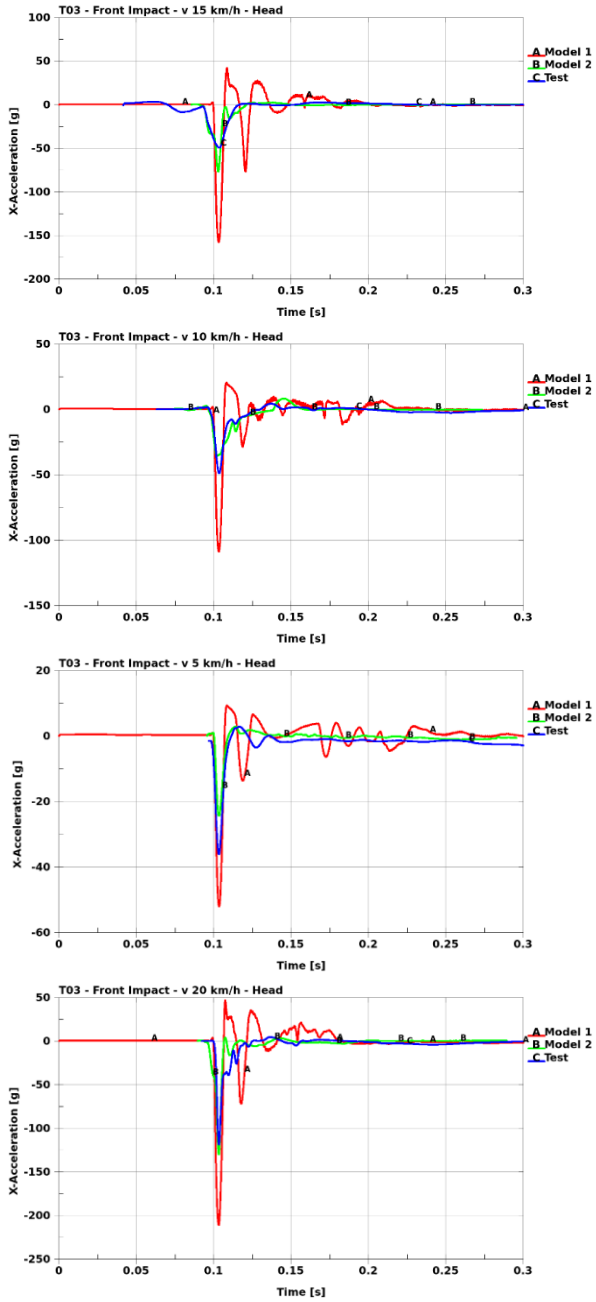

Figure 9. Tram T3, Front impact, Head acceleration in local direction X

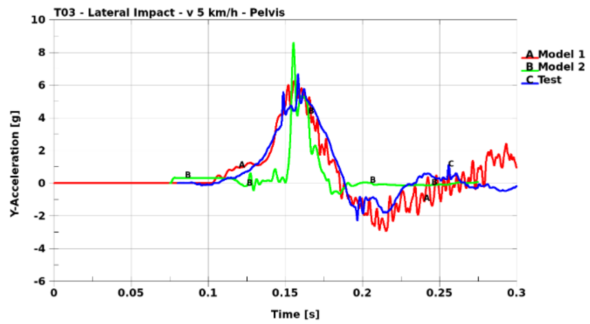

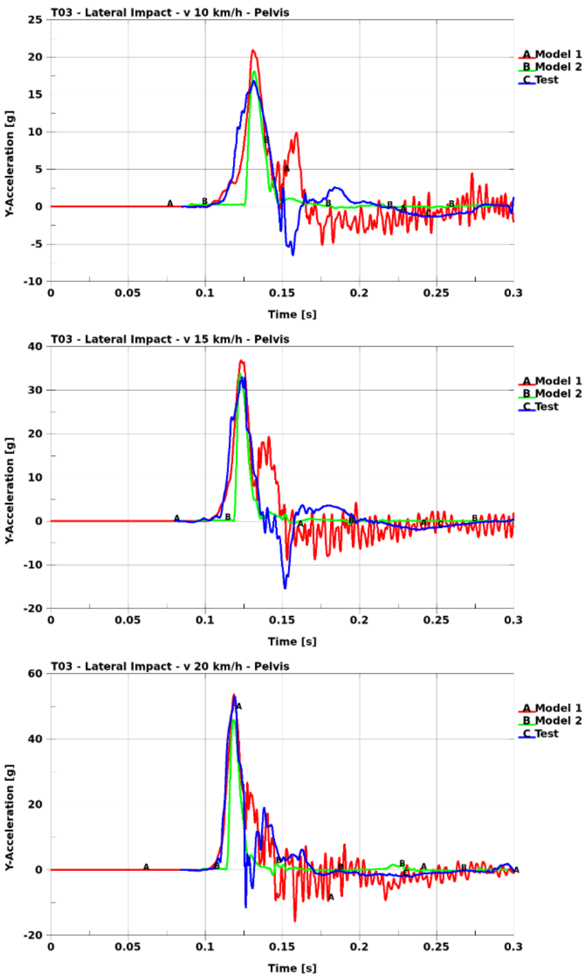

Figure 10. Tram T3, Lateral impact, Pelvis acceleration in local direction Y

Velocity [km/h]	HPC		
	Model 1	**Model 2**	**Test**
5	54	8	24
10	337	46	54
15	882	128	108
20	1731	347	272

Table 1. Tram T3, Front impact, HPC

Velocity [km/h]	Acceleration peak [g]		
	Model 1	**Model 2**	**Test**
5	52	25	37
10	108	36	49
15	156	77	49
20	210	132	118

Table 2. Tram T3, Front impact, Peak of head acceleration in local direction X

Velocity [km/h]	Correlation coefficient [-]	
	Model 1 vs. Test	**Model 2 vs. Test**
5	0.795	0.956
10	0.721	0.907
15	0.586	0.863
20	0.725	0.840

Table 3. Tram T3, Front impact, Correlation of head acceleration in local direction X

Velocity [km/h]	Acceleration peak [g]		
	Model 1	**Model 2**	**Test**
5	6	9	7
10	21	18	17
15	37	33	32
20	54	45	54

Table 4. Tram T3, Lateral impact, Peak of pelvis acceleration in local direction Y

Velocity [km/h]	Correlation coefficient [-]	
	Model 1 vs. Test	**Model 2 vs. Test**
5	0.725	0.691
10	0.705	0.772
15	0.753	0.795
20	0.828	0.838

Table 5. Tram T3, Lateral impact, Correlation of pelvis acceleration in local direction Y

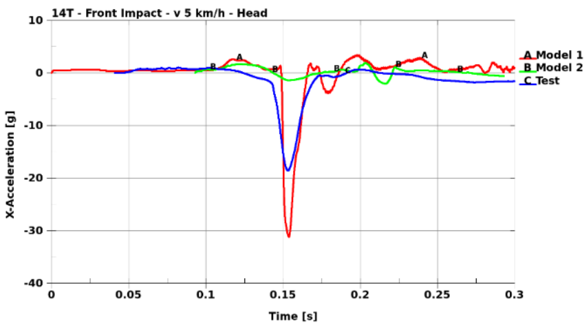

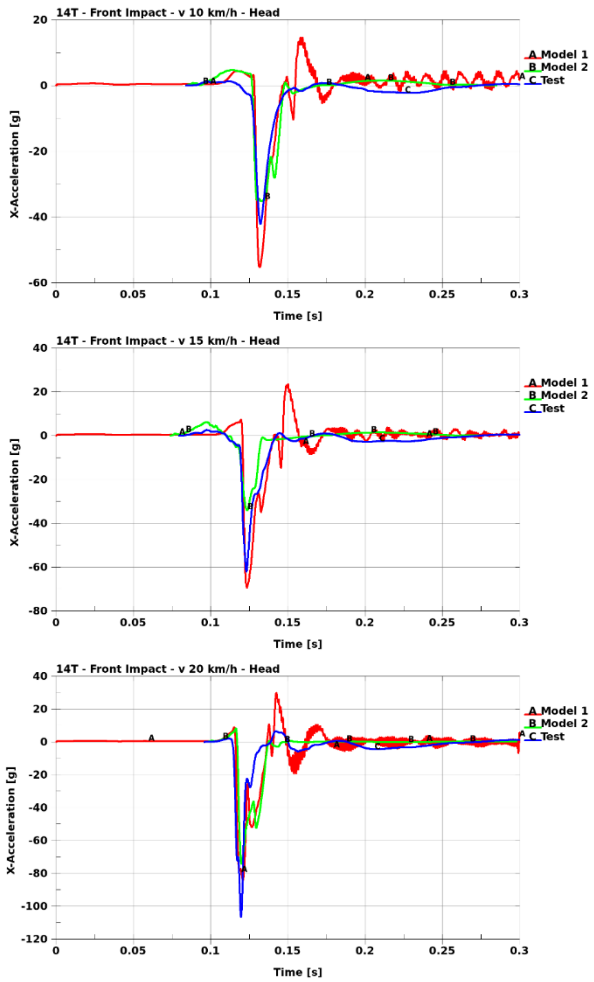

Figure 11. Tram 14T, Front impact, Head acceleration in local direction X

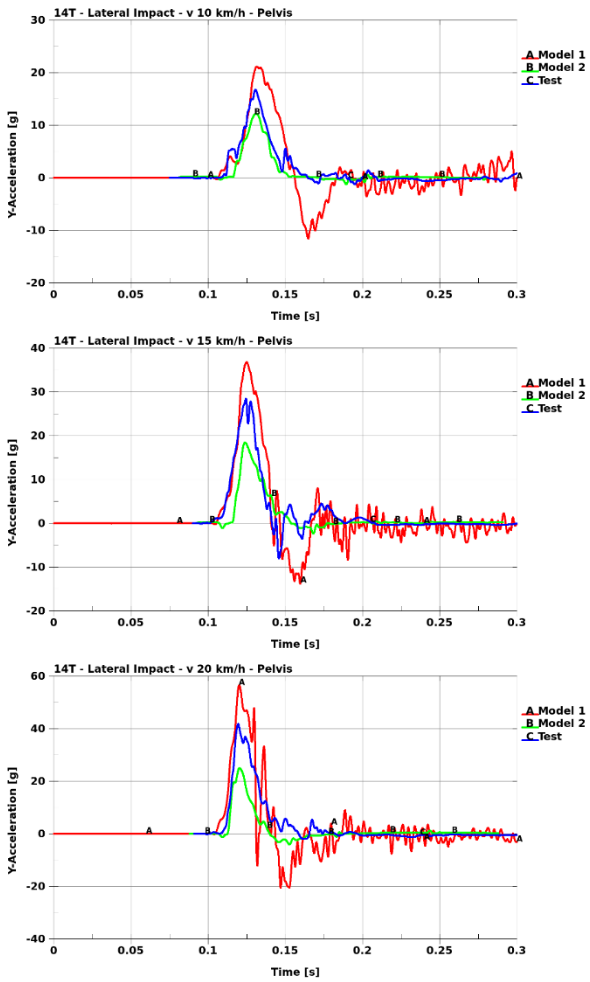

Figure 12. Tram 14T, Lateral impact, Pelvis acceleration in local direction Y

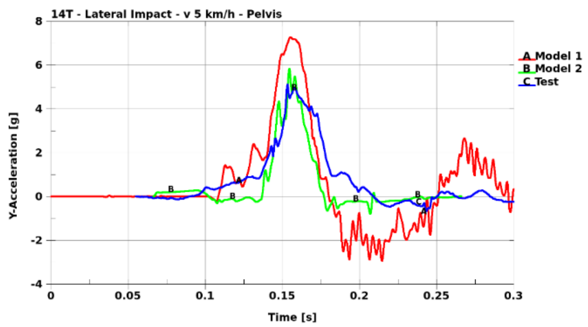

Velocity [km/h]	HPC		
	Model 1	Model 2	Test
5	27	<1	12
10	104	72	52
15	180	37	109
20	329	266	309

Table 6. Tram 14T, Front impact, HPC

Velocity [km/h]	Acceleration peak [g]		
	Model 1	Model 2	Test
5	32	2	19
10	55	35	42
15	69	34	62
20	85	74	107

Table 7. Tram 14T, Front impact, Peak of head acceleration in local direction X

Velocity [km/h]	Correlation coefficient [-]	
	Model 1 vs. Test	Model 2 vs. Test
5	0.743	0.564
10	0.754	0.921
15	0.777	0.936
20	0.597	0.679

Table 8. Tram 14T, Front impact, Correlation of head acceleration in local direction X

Velocity [km/h]	Acceleration peak [g]		
	Model 1	Model 2	Test
5	7	6	5
10	22	12	17
15	37	18	29
20	56	25	42

Table 9. Tram 14T, Lateral impact, Peak of pelvis acceleration in local direction Y

Velocity [km/h]	Correlation coefficient [-]	
	Model 1 vs. Test	Model 2 vs. Test
5	0.778	0.855
10	0.784	0.956
15	0.879	0.875
20	0.876	0.926

Table 10. Tram 14T, Lateral impact, Correlation of pelvis acceleration in local direction Y

7 DISCUSSION

The physical ATD JASTI in a sitting position (Hybrid-III50th Percentile Male ATD certificated only for front impact [LS-Dyna 2023b]) was equipped by a pedestrian kid to obtain a physical ATD in a standing position, but without certification. This brings some uncertainty about ATD behavior not only in the case of the front impact but mainly in the case of the lateral impact. The main problem is the stiffness of shoulder of the ATD. The shoulder is represented by metal lug. Comparing the human body, it is too stiff in lateral direction. The same problem is in connectin of the shoulder's lugs of the ATD. There was an attempt to compensate this imperfection via validation of the physical ATD against a live volunteer. It was done by means of small impacts series. The range of mentioned validation was, of course, limited to keeping the volunteer's health.

The LS-Dyna ATD model (LSTCH3.103008 V1. RigidFE 50th – standing) is based on the respective Hybrid III ATD. It is a BETA version without certification and brings some uncertainty about the model behavior. The standard Radioss ATD of a 50th percentile male was used and modified based on the impact tests performed. It means the model has no certification.

There are differences in the signal peak size and HPC of the acceleration obtained via tests and via simulations. Models of the tram front-end structures are based on the measured properties. This is the reason why it is expected that differences are on the side of ATD models, i.e. the local stiffness of the ATD and its simulation models are different. The stiffness of intervertebral joints can influence head acceleration in case of lateral impact when the only shoulder is in contact with the tram. The signals were shifted in time with respect to each other to have aligned their peaks of head acceleration for front impact and to have aligned their peaks of pelvis acceleration for lateral impact. There was the same time shift for all signals of each particular scenario. The peak time differences of chest and pelvis accelerations in case of front impacts and the differences of head and chest accelerations in case of lateral impact are given mainly by different positioning of ADTs (see [Jezdik 2023]) because the results are significantly sensitive to it. Moreover, it is influenced by the above-mentioned differences in stiffness, because they influence the movement of the ATD.

8 CONCLUSIONS

Experiences from tests and appropriate simulations show that it is possible to ex-post set parameters of the ATD model to achieve behavior corresponding to physical ATD. Generally, it is not possible to predict the behavior of the entire physical ATD via simulation. The simulation results are quite sensitive to the positioning and local stiffness of the ATD.

The real test realization using the entire ATD is expensive and time-consuming. Moreover, there is no standing physical ATD with certification. The repeatability of such tests is also problematic.

Due to this reason, it is recommended to evaluate the influence of the front-end tram structure on pedestrians by means of methods used in the automotive industry. It means to test the tram front end via independent body segments representing parts of the human body, see [EC Regulation 78/2009].

ACKNOWLEDGMENTS

The project was funded by Operational Programme Research, Development and Education CZ.02.1.01/0.0/0.0/16_026/0008401.

Many thanks for the excellent cooperation to the DPP staff, especially to the Chief of Technical Inspection Mgr. Martin Doubek. This project would not have been realized without them.

REFERENCES

[Altair 2023] ALTAIR ENGINEERING INC. Altair Radioss User Guide [online]. [cit. 2023-03-17]. Available from: https://help.altair.com/hwsolvers/rad/index.htm.

[CEN/TC 256 2020] Technical Committee CEN/TC 256, TR 17420, Railway applications - Vehicle end design for trams and light rail vehicles with respect to pedestrian safety, 01/2020.

[EC Regulation 78/2009] EUR-Lex. Regulation (EC) No 78/2009 of the European parliament and of the council of 14 January 2009 on the type-approval of motor vehicles with regard to the protection of pedestrians and other vulnerable road users, amending Directive 2007/46/EC and repealing Directives 2003/102/EC and 2005/66/EC. [online]. [cit. 2023-03-20]. Available from: https://eur-lex.europa.eu/legal-content/EN/ALL/?uri=CELEX:32009R0078.

[Hozman 2014] Hozman, J., Bradac, J., Kovanda, J., Neural tissue response to impact – numerical study of wave propagation at level of neural cells. Neural Network World, vol. 24, no.2, 2014 s. 157-176. ISSN 1210-0552.

[Hozman 2017] Hozman, J., Bradac, J., Kovanda, J., DG solver for the simulation of simplified elastic waves in two-dimensional piecewise homogeneous media. Neural Network World 4/2017 pg. 373-389 ISSN 1210-0552.

[Jasti 2015] CERTIFICATION, Hybrid III 50th – Dummy, No. 1125, JASTI CO., LTD., autumn 2015.

[Jasti 2023] Anthropomorphic Test Devices Dummy, JASTI CO. LTD, [online]. [cit. 2023-03-20]. Available from: https://www.jasti.co.jp/en/product/dummy.html#pedestrian.

[Jezdik 2019] Jezdik R.: Determination of Tram Windscreen Stiffness Characteristics, Conference Proceedings of CURRENT PROBLEMS IN RAIL VEHICLES - PRORAIL 2019, Zilina, 17-19 September 2019. Zilina: Scientific and Technical Society at University of Zilina, part 1, p. 283-290, ISBN 978-80-89276-58-5.

[Jezdik 2021] Jezdik R., Konopik P., Rund M., Svoboda M., Jelen K.: Determination of Material Properties of Laminates of 15T and T3 Tram Faces, Manufacturing Technology. 2021, Vol. 21, Issue 3, Page 349-359, ISSN 1213–2489, DOI: 10.21062/mft.2021.040.

[Jezdik 2023] Jezdik R., Kemka V., Kovanda J., Lopot F., Purs H., Hajkova B., Various Approaches to Reduce Consequences of Pedestrian-Tram Front End Collision, Traffics and Transportation, 2023, Vol. 35, No. 2, ISSN: 1848-4069, DOI: 10.7307/ptt.v35i2.81.

[Kovanda 2021] Kovanda J.; Rulc V., Pre-crash control strategy of driver assistance system. Neural Network World [online]. 2021, 31(1), 77–88. ISSN 23364335. Available from: doi:10.14311/NNW.2021.31.004

[LS-Dyna 2023a] Ansys LS-Dyna, [online]. [cit. 2023-03-20]. Available from: https://www.ansys.com/products/structures/ansys-ls-dyna.

[LS-Dyna 2023b] Download/Install Overview - LSDYNA, [online]. [cit. 2023-03-20]. Available from: https://lsdyna.ansys.com/download-install-overview.

[Margaritis 2007] Margaritis, D., Accident Analysis Into the Primary and Secondary Safety of City Trams in the Netherlands. Hellenic Institute of Transport (HIT), Association for European Transport and contributors. 2007.

[Safety conference 2020] Stockholm Declaration Third Global Ministerial Conference on Road Safety: Achieving Global Goals 2030 Stockholm, 19–20 February 2020

[Wismans 2000] Wismans J.; Janssen E.; Beusenberg M.; Koppens W.; Happee R.; Bovendeerd P., Injury Biomechanics (4J610) (Nr. Technical Report w5-pp3-4.3), 2000.

[Wismans 2014] Wismans J., Crash Dummies. International Course on Transportation Planning and Road Safety. IIT Dehli, India 2014.

[Tomsovsky 2019] Tomsovsky L., Literova L., Jelen K., Kubovy P., Hilmarova D., Stocek O., Lopot F., Rulc V., Hribal P., Jezdik R., Verification of Usability of the Hybrid III Dummy for Crash Tests - Pilot Experiment. Manufacturing Technology. 2022; 22(4): 477-483. DOI: 10.21062/mft.2022.052.

[Tomsovsky 2022] Tomsovsky L., Lopot F., Kubovy P., Jezdik R., Hajkova B., Rulc V., Jelen K., Tram-pedestrian collisions: The severity of head injuries due to secondary impact with the surrounding infrastructure (ground). 2022 International Conference on Electrical, Computer, Communications and Mechatronics Engineering (ICECCME), Maldives. 2022, pp. 1-6. DOI: 10.1109/ICECCME55909.2022.9988616.

CONTACTS:

Ing. Roman Jezdik
VUKV a. s., Research, development, and testing of railway rolling stock
Department of Structural analysis of Vehicles
Bucharova 1314/8, Prague 5, 158 00, Czech Republic
jezdik@vukv.cz